An Analytic Method of Determining a Critical Cable Spacing for Acceptable Crosstalk

Pei Xiao, Wan-Wei Ran, and Ping-An Du*

School of Mechanical and Electrical Engineering
University of Electronic Science and Technology of China, Chengdu 611731, China
xiaopei_uestc@sina.cn, rww4gz@163.com, dupingan@uestc.edu.cn*

Abstract ─ Some wiring rules have been used to prevent crosstalk in industrial application, but the technical rationale is not clear. This paper aims at proposing an analytic method of determining a critical cable spacing for acceptable crosstalk. First of all, we derive a calculation function of crosstalk with cable spacing. Then, we discuss about the crosstalk characteristics according to the crosstalk function and its curve. On this basis, we define the critical cable spacing via a critical point on the curve and explain physical meaning of the critical point by use of the fringe field around the victim cable. After that, we analyze the influence of wiring parameters on the critical cable spacing. Finally, we conduct an experiment to validate the proposed method of the critical cable spacing.

Index Terms ─ Critical cable spacing, critical point, crosstalk, wiring parameters.

I. INTRODUCTION

Crosstalk interference is a phenomenon affecting signals propagated in cables and has a close relationship with cable spacing. The aggressor cable may produce induced degradation or failures on the adjacent victim cable due to the coupling of fringe electric field, which may arouse overall electromagnetic compatibility problem of the whole electronic system [1-4]. Some rules have been used for guiding wiring of adjacent cables to prevent crosstalk [5-7], but the technical rationale is not clear. Thus, analytic determination of critical cable spacing is an important issue in industrial application.

Previous work mainly concentrated on the methods of evaluating crosstalk [8-10]. Numerical simulation has been widely adopted to obtain the coupled crosstalk, but it requires a reliable model of cable harness [11-13]. Compared with numerical simulation in calculating induced interference on the victim cable, analytic technique performs better computing efficiency and consumes less computation resources. As twisted pair cable is generally applied to transmit information from a piece of equipment to another, many works have been published on modeling of predicting the coupling problem on twisted cables [14-16]. For the discontinuities such as via, bends and changes in geometry of a multiconductor transmission lines (MTLs) system, some researchers apply the scalar and vector potentials associated with boundary conditions to obtain non-uniform transmission line equation and crosstalk for conductors [17-18]. Some others used the cascaded transmission line theory to deal with crosstalk calculation of conductors with bends and varying size [19-20]. Recently measurement-based modeling techniques are presented to determine the crosstalk parameters of cables [21-22], which helps to give a worst-case estimation of crosstalk.

A simple and efficient way of controlling crosstalk is to keep the cables farther apart, but the question is how far apart enough, seldom analytic work about cable spacing rules are studied so far. Hence, this paper proposed an analytic method to deal with the determination of critical cable spacing for acceptable crosstalk so that an effective way of wiring can be formed. Firstly, we derived an analytic calculation formula of crosstalk with cable spacing, which contains the determination of parasitic capacitive and inductive and solution of coupled crosstalk equations. Then, we discussed about the crosstalk characteristics according to the crosstalk function and its curve. On this basis, we defined the critical cable spacing via a critical point on the curve and explained physical meaning of the critical point by use of the fringe field around the victim cable, in addition, analyzed the influence of wiring parameters on the critical cable spacing. Finally, we conducted an experiment to validate the proposed calculation method of the critical cable spacing. This work can provide an analytic way of wiring rules.

II. DERIVATION OF THE FUNCTION OF CROSSTALK WITH CABLE SPACING

A. Derivation of crosstalk calculation

A transmission line model is often used to describe the crosstalk phenomenon between two parallel cables, as illustrated in Fig. 1, where the aggressor and victim

Submitted On: January 16, 2019
Accepted On: January 3, 2020

cables are placed over a perfectly conducting ground plane and excited by voltage sources, Z represents terminal loads on both cables, L_{ji} and C_{ji} $(j=1,2)$ are the per unit length self-inductance and self-capacitance, L_i and C_i the mutual inductance and capacitance. The crosstalk problem arises from the sum of mutual capacitive and inductive coupling noise propagating in the length direction along the victim cable.

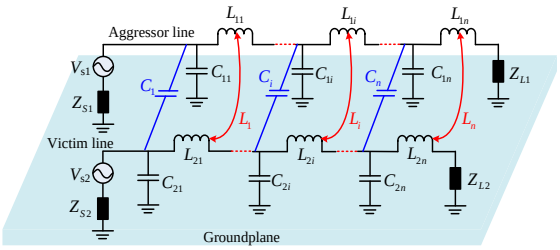

Fig. 1. Schematic for crosstalk coupling of two conductors.

The calculation formula of inductance matrix $\hat{L}$ can be written as [19]:

$$\hat{L}=\begin{bmatrix} \frac{\mu_0}{2\pi}\ln\left(\frac{2h_A}{r_A}\right) & \frac{\mu_0}{4\pi}\ln\left(1+\frac{4h_Ah_B}{S^2}\right) \\ \frac{\mu_0}{4\pi}\ln\left(1+\frac{4h_Ah_B}{S^2}\right) & \frac{\mu_0}{2\pi}\ln\left(\frac{2h_B}{r_B}\right) \end{bmatrix}, \tag{1}$$

where S is the spacing between two cables, r_A and r_B the radius of two cable, Δr_A and Δr_B the dielectric thickness, h_A and h_B the height to the ground, μ_0 the permeability for free space.

The calculation formula of capacitance matrix $\hat{C}$ can be given as [19]:

$$\hat{C}=\begin{bmatrix} a_{11} & a_{12} \\ a_{21} & a_{22} \end{bmatrix}^{-1}, \tag{2}$$

where a_{11}, a_{12}, a_{21} and a_{22} are defined by:

$$\begin{cases} a_{11}=\dfrac{1}{2\pi\varepsilon_0}\left(\dfrac{1}{\varepsilon_r}\ln\dfrac{1}{r_A}+\varepsilon_e\ln\dfrac{1}{r_A+\Delta r_A}-\ln\dfrac{1}{2h_A}\right) \\ a_{12}=a_{21}=\dfrac{1}{4\pi\varepsilon_0}\ln\left(1+\dfrac{4h_Ah_B}{S^2}\right) \\ a_{22}=\dfrac{1}{2\pi\varepsilon_0}\left(\dfrac{1}{\varepsilon_r}\ln\dfrac{1}{r_B}+\varepsilon_e\ln\dfrac{1}{r_B+\Delta r_B}-\ln\dfrac{1}{2h_B}\right) \end{cases}, \tag{3}$$

where ε_0 is the permittivity for free space, ε_r the relative dielectric constant and $\varepsilon_e=(\varepsilon_r-1)/\varepsilon_r$.

According to the multi-conductor transmission lines theory, the induced voltage and current along the cables in frequency domain can be written as:

$$\frac{\mathrm{d}^2\hat{V}(z)}{\mathrm{d}z^2}=\hat{Z}\hat{Y}\hat{V}(z), \tag{4}$$

$$\frac{\mathrm{d}^2\hat{I}(z)}{\mathrm{d}z}=\hat{Y}\hat{Z}\hat{I}(z), \tag{5}$$

where $\hat{V}(z)$ and $\hat{I}(z)$ are the voltage and current matrix, $\hat{Z}=j\omega\hat{L}$ and $\hat{Y}=j\omega\hat{C}$ the impedance and admittance matrix.

To solve the coupled (4) and (5), a decoupling approach is applied to obtain $\hat{V}(z)$ and $\hat{I}(z)$. Thus, the key problem is how to find the transformational matrix $\hat{T}_V$ and $\hat{T}_I$ which satisfy:

$$\hat{V}=\hat{T}_V\hat{V}_m, \tag{6}$$

$$\hat{I}=\hat{T}_I\hat{I}_m, \tag{7}$$

where $\hat{V}_m$ and $\hat{I}_m$ are diagonal matrix and denote mode voltage and current propagating along the cables. $\hat{T}_V$ and $\hat{T}_I$ transform the off-diagonal matrix $\hat{Z}\hat{Y}$ and $\hat{Y}\hat{Z}$ to the diagonal matrix $\hat{\gamma}$ which satisfy $\hat{T}_V^{-1}\hat{Z}\hat{Y}\hat{T}_V=\hat{T}_I^{-1}\hat{Y}\hat{Z}\hat{T}_I=\hat{\gamma}^2$.

Then, we can obtain the decoupled voltage and current equations as follows:

$$\frac{\mathrm{d}^2V_m(z)}{\mathrm{d}z^2}=\hat{\gamma}^2\hat{V}_m(z), \tag{8}$$

$$\frac{\mathrm{d}^2\hat{I}_m(z)}{\mathrm{d}z^2}=\hat{\gamma}^2\hat{I}_m(z). \tag{9}$$

Consequently, the solution of mode voltage $\hat{V}_m$ and current $\hat{I}_m$ at position z along the cables can be written as:

$$\hat{V}_m(z)=\hat{e}^{-\gamma z}\hat{V}_m^{+}+\hat{e}^{\gamma z}\hat{V}_m^{-}, \tag{10}$$

$$\hat{I}_m(z)=\hat{e}^{-\gamma z}\hat{I}_m^{+}-\hat{e}^{\gamma z}\hat{I}_m^{-}, \tag{11}$$

where $\hat{V}_m^{+}$ and $\hat{I}_m^{+}$ are the forward transmission mode voltage and current, while $\hat{V}_m^{-}$ and $\hat{I}_m^{-}$ the backward transmission mode voltage and current matrix. Transmission coefficient matrix $\hat{e}^{\pm\gamma z}$ equals to:

$$\hat{e}^{\pm\gamma z}=\begin{bmatrix} e^{\pm\gamma_1 z} & 0 \\ 0 & e^{\pm\gamma_2 z} \end{bmatrix}. \tag{12}$$

According to the calculation results of mode voltage

$\hat{V}_m$ and mode current $\hat{I}_m$, we obtain the crosstalk voltage and current:

$$\hat{I}(z) = \hat{T}_I \left(e^{-\gamma z} \hat{I}_m^+ - e^{\gamma z} \hat{I}_m^- \right), \tag{13}$$

$$\hat{V}(z) = \hat{Y}^{-1} \hat{T}_I \hat{\gamma} \left(e^{-\gamma z} \hat{I}_m^+ + e^{\gamma z} \hat{I}_m^- \right). \tag{14}$$

Assuming the conductors only contain voltage source excitation on both terminals, (13) and (14) satisfy:

$$\hat{V}(0) = \hat{V}_S - \hat{Z}_S \hat{I}(0), \tag{15}$$

$$\hat{V}(L) = \hat{V}_L + \hat{Z}_L \hat{I}(L), \tag{16}$$

where $\hat{V}(0)$ and $\hat{V}(L)$ represent the terminal voltage, $\hat{I}(0)$ and $\hat{I}(L)$ the terminal current.

Inserting (13) and (14) at z=0 into (15), we obtain:

$$\hat{Y}^{-1} \hat{T}_I \hat{\gamma} (\hat{I}_m^+ + \hat{I}_m^-) = \hat{V}_S - \hat{Z}_S \hat{T}_I (\hat{I}_m^+ - \hat{I}_m^-). \tag{17}$$

Inserting (13) and (14) at z=L into (16), we obtain:

$$\hat{Y}^{-1} \hat{T}_I \hat{\gamma} (\hat{e}^{-\gamma L} \hat{I}_m^+ + \hat{e}^{\gamma L} \hat{I}_m^-) = \hat{V}_L + \hat{Z}_L \hat{T}_I (\hat{e}^{-\gamma L} \hat{I}_m^+ - \hat{e}^{\gamma L} \hat{I}_m^-). \tag{18}$$

(17) and (18) can be written as a matrix equation:

$$\begin{bmatrix} \hat{Y}^{-1} \hat{T}_I \hat{\gamma} + \hat{Z}_S \hat{T}_I & \hat{Y}^{-1} \hat{T}_I \hat{\gamma} - \hat{Z}_S \hat{T}_I \\ \left(\hat{Y}^{-1} \hat{T}_I \hat{\gamma} - \hat{Z}_L \hat{T}_I \right) \hat{e}^{-\gamma L} & \left(\hat{Y}^{-1} \hat{T}_I \hat{\gamma} + \hat{Z}_L \hat{T}_I \right) \hat{e}^{-\gamma L} \end{bmatrix} \begin{bmatrix} \hat{I}_m^+ \\ \hat{I}_m^- \end{bmatrix} = \begin{bmatrix} \hat{V}_S \\ \hat{V}_L \end{bmatrix}. \tag{19}$$

Through this matrix equation, we can obtain $\hat{I}_m^+$ and $\hat{I}_m^-$. Substituting the calculated results of $\hat{I}_m^+$ and $\hat{I}_m^-$ into (13) and (14), we can obtain the crosstalk $\hat{I}(z)$ and $\hat{V}(z)$ along the victim cable, which is used for the derivation of critical cable spacing.

B. Definition of the function of crosstalk with cable spacing

Define matrix $\hat{M}$:

$$\hat{M} = \begin{bmatrix} \hat{Y}^{-1} \hat{T}_I \hat{\gamma} + \hat{Z}_S \hat{T}_I & \hat{Y}^{-1} \hat{T}_I \hat{\gamma} - \hat{Z}_S \hat{T}_I \\ \left(\hat{Y}^{-1} \hat{T}_I \hat{\gamma} - \hat{Z}_L \hat{T}_I \right) \hat{e}^{-\gamma L} & \left(\hat{Y}^{-1} \hat{T}_I \hat{\gamma} + \hat{Z}_L \hat{T}_I \right) \hat{e}^{-\gamma L} \end{bmatrix}^{-1} = \begin{bmatrix} \hat{A} & \hat{B} \\ \hat{C} & \hat{D} \end{bmatrix}, \tag{20}$$

where matrix A, B, C and D are all the function of cable spacing S. Letting,

$\hat{A} = f_1(S)$, $\hat{B} = f_2(S)$, $\hat{C} = f_3(S)$ and $\hat{D} = f_4(S)$, then,

$$\hat{I}_m^+ = f_1(S) \hat{V}_S + f_2(S) \hat{V}_L, \tag{21}$$

$$\hat{I}_m^- = f_3(S) \hat{V}_S + f_4(S) \hat{V}_L. \tag{22}$$

Inserting (21) and (22) into (13) and (14) respectively, the calculation formula of $\hat{I}(z,S)$ and $\hat{V}(z,S)$ at position z with cable spacing of S can be modified as:

$$\hat{I}(z,S) = \hat{T}_I \left[\hat{e}^{-\gamma z} \left(f_1(S) \hat{V}_S + f_2(S) \hat{V}_L \right) - \hat{e}^{\gamma z} \left(f_3(S) \hat{V}_S + f_4(S) \hat{V}_L \right) \right], \tag{23}$$

$$\hat{V}(z,S) = \hat{Y}^{-1} \hat{T}_I \hat{\gamma} \left[\hat{e}^{-\gamma z} \left(f_1(S) \hat{V}_S + f_2(S) \hat{V}_L \right) + \hat{e}^{\gamma z} \left(f_3(S) \hat{V}_S + f_4(S) \hat{V}_L \right) \right]. \tag{24}$$

Through (23) and (24), we can analyze the influence of cable spacing on crosstalk voltage and current.

C. Numerical validation of crosstalk calculation

To validate the addressed analytic calculation of crosstalk between adjacent cables, a two copper cables model is constructed, as illustrated in Fig. 2. The two cables have a core radius of 0.7 mm, a dielectric insulation layer thickness of 0.7 mm, a height of 10 mm to the ground, and a spacing of 25 mm. The aggressor cable is excited by a 1 V voltage over frequency (0,500MHz), and all terminal impedance are 50Ω.

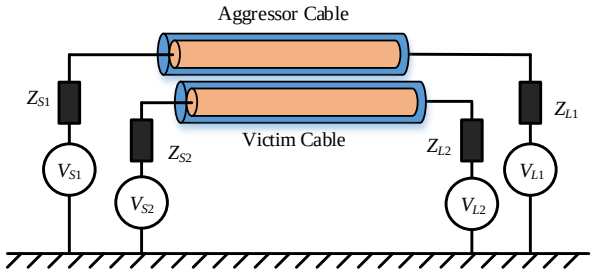

Fig. 2. Voltage source excitation on the cables' terminals.

In this paper, a full-analysis commercial software CST based on transmission line matrix (TLM) technique is utilized to provide a numerical validation. By using 2D(TL) modeling technique, the equivalent circuit of cable model is obtained and then the crosstalk is calculated by using AC combine results solver. The solid curves in Figs. 3 (a) and (b) respectively show the calculation results of induced voltage on the near and far end of the victim cable by the analytic method, while the dotted curves demonstrate the results from CST simulation.

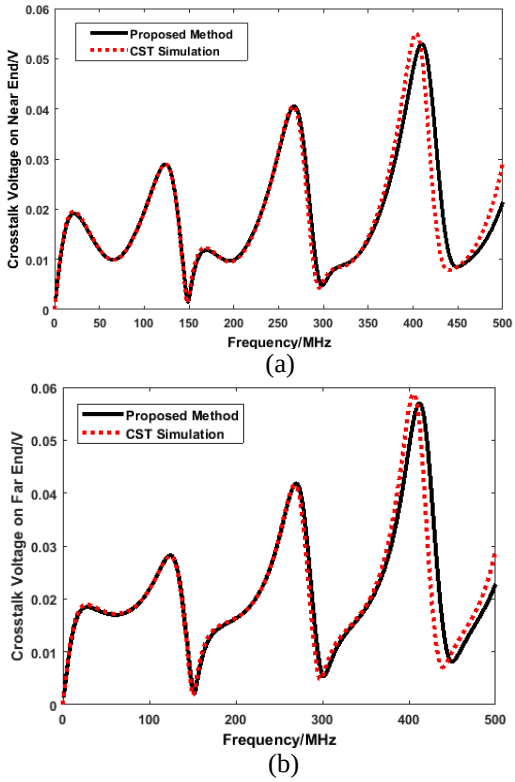

Fig. 3. Comparison results of crosstalk voltage on victim cable: (a) near end; (b) far end.

A good agreement between the analytic and simulation results establishes the validation of crosstalk calculation formula. A little difference between two curves can be seen at higher frequency, which may be caused by the error during the analytic calculation of capacitance at higher frequency due to dielectric insulation layer.

III. DISCUSSION

A. Definition of critical cable spacing

According to (24), we can draw out the curve of near crosstalk voltage $\hat{V}(z,S)$ with cable spacing S by changing S from 25 mm to 180 mm at frequency 276MHz, as illustrated in Fig. 4 (a). The curve shows that crosstalk voltage decreases with the increased S, especially decreases very sharply at the beginning but begins to flatten when S reaches a certain value which we define as the critical point. As illustrated in Fig. 4 (b), the variation of crosstalk at different frequency point is consistent with the cable spacing. So, the choice for frequency 274 MHz in our method is unintentional and the proposed method can be extended to other frequency points.

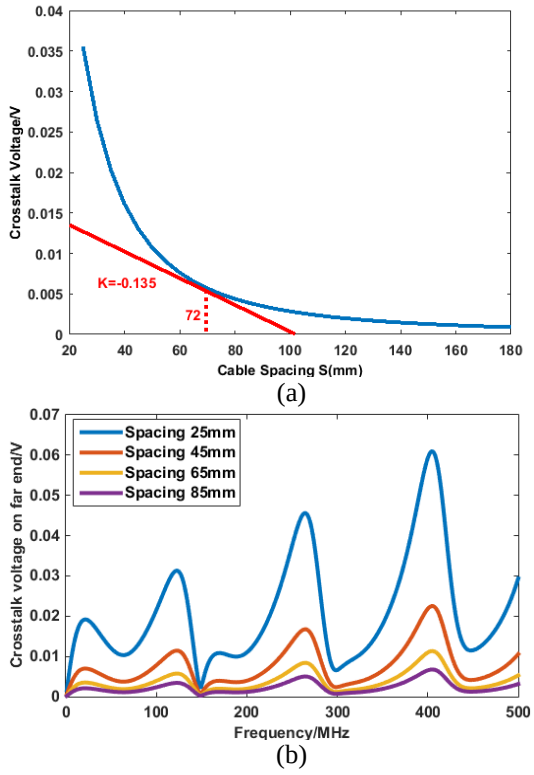

Fig. 4. Crosstalk: (a) crosstalk voltage with cable spacing from 20 mm to 180 mm; (b) crosstalk voltage at different cable spacing.

Since the derivative reflects the change rate of a function with an independent variable, taking the derivation of the crosstalk voltage function (24) to variable S, we obtain:

$$K = \frac{\mathrm{d}\left(\hat{V}(z,S)\right)}{\mathrm{d}S}. \tag{25}$$

The function K describes the change rate of crosstalk voltage with S. Here, we define S_0 at the critical point in Fig. 4 as the critical cable spacing. Therefore, S_0 satisfy that the change rate of crosstalk begins to reduce slowly enough when $S > S_0$. The determination of S_0 refer to the difference value of K between evenly spaced adjacent points. The choice of value for K is based on the trend of the slope between evenly spaced adjacent points. When the slope difference change little, we take the intermediate value to be K at the critical point. For example, a series of derivative value K at S of (25, 35, 45, 55, 65, 75, 85, 95) mm correspond to (-2.60, -1.02, -0.50, -0.29, -0.18, -0.12, -0.09, -0.06) respectively. The calculated results denote a little

difference of K starting from the range (-0.18, -0.12). Taking the intermediate value to be K at the critical point, namely K = -0.135, the corresponding S_0 = 72mm, as illustrated in Fig. 3. Thus, the analytic calculation process of S_0 can be summarized as the following steps:

a) Definition of the function of crosstalk with cable spacing;

b) Determination of the value of K at the critical point according to its derivative;

c) Calculation of S_0 by substituting K to the derivative function.

B. Physical interpretation of critical cable spacing

If ignoring the field reflection effect of victim cable, the fringe E-field generated by a dipole $I(z)\mathrm{d}z$ at position z along the aggressor cable in Cartesian coordinate can be defined by:

$$\begin{cases} dE_x = e_x\left\{-j\dfrac{I(z)dz}{4\pi\omega\varepsilon_0}\dfrac{e^{-jkr}}{r^2}\sin\theta\cos\theta\cos\varphi[3jk-rk^2+\dfrac{3}{r}]\right\} \\ dE_y = e_y\left\{-j\dfrac{I(z)dz}{4\pi\omega\varepsilon_0}\dfrac{e^{-jkr}}{r^2}\sin\theta\cos\theta\sin\varphi[3jk-rk^2+\dfrac{3}{r}]\right\} \\ dE_z = e_z\left\{j\dfrac{I(z)dz}{4\pi\omega\varepsilon_0}\dfrac{e^{-jkr}}{r^2}[(jk-rk^2+\dfrac{1}{r})\sin^2\theta-(2jk+\dfrac{2}{r})\cos^2\theta]\right\} \end{cases}, \quad (26)$$

where $k=\omega\sqrt{\mu_0\varepsilon_0}$ is propagation constant, ω angular frequency, r radiation distance, θ and φ the radiation angles of the fringe fields.

Then, the E-field generated by the aggressor cable can be obtained by adding up the sum of the contribution from each dipole to the field components, that is:

$$E = e_x\int_0^l dE_x + e_y\int_0^l dE_y + e_z\int_0^l dE_z \,. \quad (27)$$

Figure 5 gives the mechanism of E-field coupling to conductor. The victim conductor is illuminated by a uniform plane-wave field characterized by strength of electric field vector E and arbitrary incidence (θ, ψ) and polarization η angles, as shown in the following figure. The coupling crosstalk V_{cp} can be written as [23]:

$$V_{cp} = 2Eh\left\{F\frac{\gamma_0 e^{-\hat{\gamma}_0 L}-\gamma_0\cosh(\gamma_0 L)+\hat{\gamma}_0\sinh(\gamma_0 L)}{\gamma_0\sinh(\gamma_0 L)}-G\right\}, \quad (28)$$

where

$$F=\frac{\cos\theta(\cos\psi\cos\theta\cos\eta+\sin\psi\sin\eta)}{1-\sin^2\theta\cos^2\psi}, \quad (29)$$

$$G=\sin\theta\cos\eta\,, \quad (30)$$

$$\hat{\gamma}_0=\gamma_0\sin\theta\cos\psi\,. \quad (31)$$

From (27)-(31), we can know that the induced crosstalk is related to the incident E-field. For crosstalk problem between two conductors, the fringe coupling E-field is generated by the aggressor cable. Therefore, we can explain the influence of cable spacing on the fringe fields around the victim cable. The detailed interpretation can be founded in the reference [23].

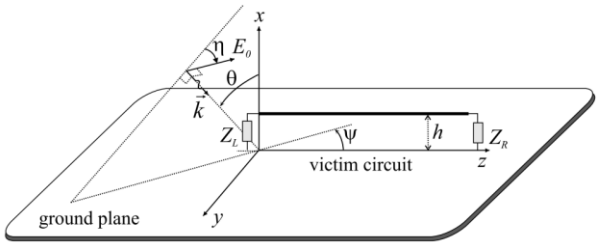

Fig. 5. Principle drawing of the victim circuit illuminated by a uniform plane-wave EM field: definition of wave angles [23].

Figure 6 shows the relationship between E-field and radiation distance r from 25 mm to 180 mm at frequency 420MHz. From Fig. 6, we can see that the radiated E-field reduces quickly at the beginning of the curve, then begins to flatten when spacing reaches a value. This change rule is consistent with that of crosstalk. As crosstalk voltage is induced by the fringe E-fields, Fig. 5 gives a reasonable interpretation of determination of the critical cable spacing.

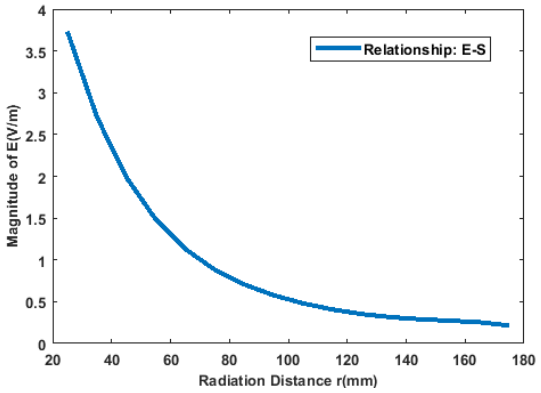

Fig. 6. Relationship between radiation distance r and E-field radiated from the aggressor cable.

From the crosstalk curve in Fig. 4 and E-field curve in Fig. 6, we can see that the basic trend of the two curves is the same. However, it should be noted that the change rate of E-field with distance is not strictly the same as that of crosstalk, especially at low frequencies. This may be caused by the magnetic field.

C. Influence of wiring parameters on critical cable spacing

According to the derivation of crosstalk calculation, the critical cable spacing is related to wiring parameters. Figure 7 (a) and Fig. 7 (b) show the influence of cable

length and height to the ground on critical cable spacing, which are calculated at the resonance frequency 276MHz. The two figures indicate obviously that the longer of the cable or the higher to the ground, the greater the critical cable spacing. This phenomenon can be explained by the coupled fringe E-field, that is, the longer of the cable and the higher to the ground, the more fringe E-field coupled and the greater voltage induced.

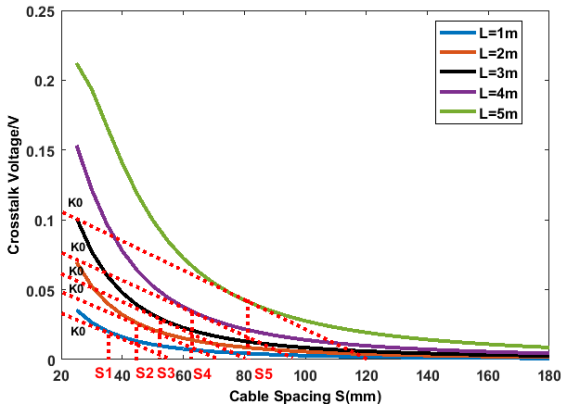

(a)

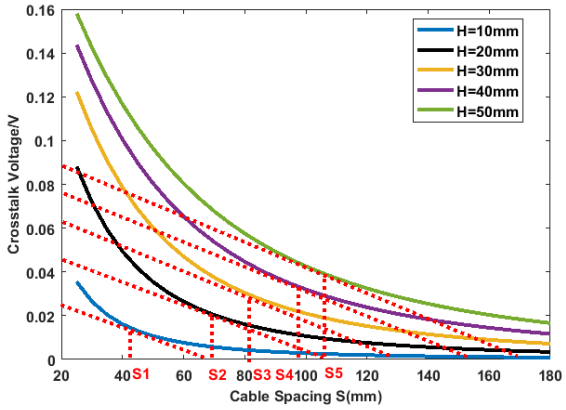

(b)

Fig. 7. Influence of wiring parameters on critical cable spacing: (a) cable length; (b) cable height to the ground.

IV. EXPERIMENTAL VALIDATION OF CRITICAL CABLE SPACING

To validate the analytic calculation of the critical cable spacing, we test the crosstalk of two cables based on S_{21} parameter measurement in a well-controlled test setup. Define the incident voltage U_0 and reflected voltage U_1, equals to:

$$S_{21} = \frac{U_1}{U_0}. \tag{32}$$

Therefore, we can measure the S_{21} of a two cables system to obtain the crosstalk on the victim cable by injecting a voltage U_0 into the aggressor cable.

The diagram of the measurement system is shown in Fig. 8, where a Keysight FieldFox Analyzers N9913A (it can be used as Vector Network Analyzer and Spectrum Analyzer and its test frequency band ranges from 30 kHz to 4 GHz) is adopted to measure S_{21} on the near end of the victim wire, and the tested cable has a core radius of 0.7 mm, a dielectric insulation layer of 0.7 mm and 300 mm long and 10 mm high above a ground reference which is a finite metallic plane with a length of 1m and width of 0.5 m. Two cables are connected to the analyzer through SMA connectors. The impedance of matching resistor at each terminal of the cable is 50 Ω .

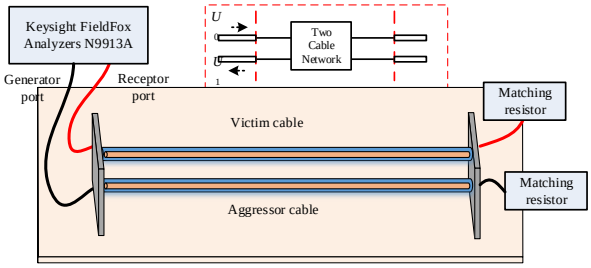

Fig 8. Principle diagram of S_{21} parameter test.

The experimental test picture is illustrated in Fig. 9. Measurements were performed over (30KHz, 200MHz) by moving the aggressor cable from 25mm to 145mm with a distance interval of 20mm and recording S_{21} of each step.

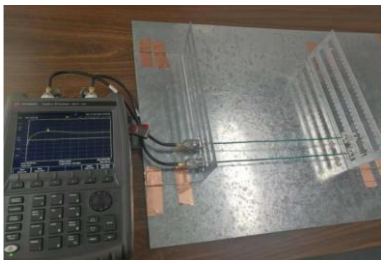

Fig. 9. Experimental test picture of S_{21}.

Figure 10 (a) gives the measurement results of S_{21} at different cable spacing. Figure 10 (b) is the fitted curve of S_{21} with cable spacing at the first resonance frequency 35 MHz, which demonstrates the relationship between S_{21} and cable spacing. Figure 10 denotes that the greater the cable spacing, the slower the change rate of S_{21}. The fitted function of the relationship between S_{21} and cable spacing are written as:

$$F = \alpha S^b + \beta, \tag{33}$$

where the coefficient α = 86.12, β = -44.93, b = -0.3746.

By taking the derivative of F to S and making the derived function be the critical derivative K_0, we can obtain the corresponding critical cable spacing S_0. For

example, inserting K_0 = -0.135 into the derivative of F, the calculation result of critical cable spacing S_0 is 54 mm. A little difference of the S_0 exists between measurement and analytic results at K_0 = -0.135, which is caused by the experimental cable model due to the inevitable bending in the wiring process. But the trend of the measurement curve in Fig. 10 establishes the validation of proposed calculation method of critical cable spacing.

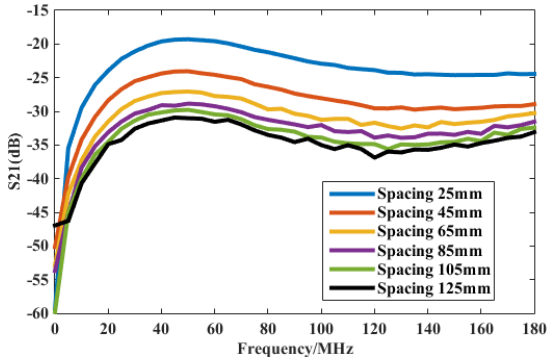

(a)

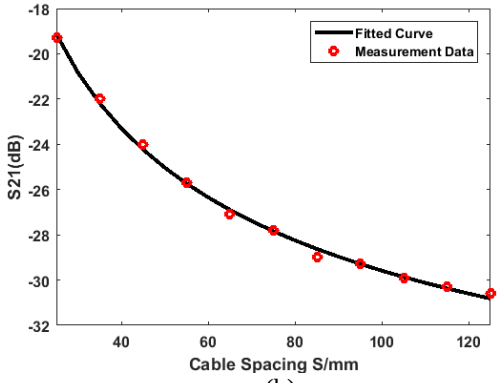

(b)

Fig. 10. Experimental measurement of S_{21}: (a) S_{21} at different cable spacing, and (b) the measurement data of S_{21} and its fitted curve at resonance frequency 35MHz.

V. CONCLUSION

To deal with the relationship between crosstalk and cable spacing, this paper proposed an analytic method of determining the critical cable spacing for acceptable crosstalk. First of all, a calculation function of crosstalk with cable spacing was derived, which gave more insight in crosstalk with cable spacing. Then, the crosstalk characteristic was discussed according to the crosstalk function and its curve. On this basis, the critical cable spacing was defined via a critical point on the curve and a physical explanation of the critical point was given by use of the fringe E-field around the victim cable, in addition, wiring parameters of cable length and height was studied to analyze the influence on critical cable spacing. Finally, an experiment based on S_{21} parameter measurement in a well-controlled test setup was carried out to validate the proposed calculation method of the critical cable spacing.

From the analytic process of critical cable spacing, it can be expected that the universality of crosstalk versus separation curve can be applied for more complex cases such as multi-wire and shielded cables. The difference is the way of calculating crosstalk, but the law of crosstalk varying with the spacing is in a similar way. This work contributed to wiring rules of cables in industrial application.

ACKNOWLEDGMENT

This project is supported by the National Natural Science Foundation of China (Grant No. 51675086).

REFERENCES

[1] S. Sun, G. Liu, J. L. Drewniak, et al., "Hand-assembled cable bundle modeling for crosstalk and common-mode radiation prediction," [J]. *IEEE Transactions on Electromagnetic Compatibility*, vol. 49, no. 3, pp. 708-718, 2007.

[2] J. Wang, "Leaky coaxial cable with circular polarization property," [J]. *IEEE Transactions on Antennas & Propagation*, vol. 59, no. 2, pp. 682-685, 2011.

[3] H. K. Dong and H. J. Eom, "Radiation of a leaky coaxial cable with narrow transverse slots," [J]. *IEEE Transactions on Antennas & Propagation*, vol. 55, no. 1, pp. 107-110, 2007.

[4] B. L. Nie, P. A. Du, Y. T. Yu, et al., "Study of the shielding properties of enclosures with apertures at higher frequencies using the transmission-line modeling method," [J]. *IEEE Transactions on Electromagnetic Compatibility*, vol. 53, no. 1, pp. 73-81, 2011.

[5] EN 50174-1, Integrated Standards for Telecommunications cabling installation. [S]. 2018.

[6] IEC 61000-5-2, Electromagnetic Compatiblity (EMC)-Part 5: Installation and mitigation guidelines-Section 2: Earthing and Cabling. [S]. 1997.

[7] IET. IET wiring regulations (BS 7671:2008 incorporating amendment number 3:2015). [S]. 2015.

[8] M. Sung, W. Ryu, H. Kim, et al., "An efficient crosstalk parameter extraction method for high-speed interconnection lines," [J]. *IEEE Transactions on Advanced Packaging*, vol. 23, no. 2, pp. 148-155, 2000.

[9] A. Palczyńska, A. Wymysłowski, T. Bieniek, et al., "Crosstalk phenomena analysis using electromagnetic wave propagation by experimental an numerical simulation methods," [C]. *International Conference on Thermal, Mechanical and Mulit-Physics Simulation and Experiments in Micro-electronics and Microsystems. IEEE*, 2014:1-10.

[10] L. Ding, D. Blaauw, and P. Mazumder, "Accurate

crosstalk noise modeling for early signal integrity analysis," [J]. *IEEE Transactions on Computer-Aided Design of Integrated Circuits and Systems*, vol. 22, no. 5, pp. 627-634, 2003.

[11] Y. Massoud and J. White, "Simulation and modeling of the effect of substrate conductivity on coupling inductance and circuit crosstalk," [J]. *Very Large Scale Integration Systems IEEE Transactions on*, vol. 10, no. 3, pp. 286-291, 2002.

[12] P. Lafata and P. Jares, "Analysis of simulation methods for far-end crosstalk cancellation," [J]. *Radioengineering*, vol. 20, no. 1, pp. 143-150, 2011.

[13] Z. Li, L. L. Liu, J. Yan, et al., "An efficient simplification scheme for modeling crosstalk of complex cable bundles above an orthogonal ground plane," [J]. *IEEE Transactions on Electromagnetic Compatibility*, vol. 55, no. 5, pp. 975-978, 2013.

[14] C. Jullien, P. Besnier, M. Dunand, et al., "Advanced modeling of crosstalk between an unshielded twisted pair cable and an unshielded wire above a ground plane," [J]. *IEEE Transactions on Electromagnetic Compatibility*, vol. 55, no. 1, pp. 183-194, 2013.

[15] G. Spadacini, F Grassi, F. Marliani, et al., "Transmission-line model for field-to-wire coupling in bundles of twisted-wire pairs above ground," [J]. *IEEE Transactions on Electromagnetic Compatibility*, vol. 56, no. 6, pp. 1682-1690, 2014.

[16] P. Kirawanich, J. R. Wilson, N. E. Islam, et al., "Minimizing crosstalks in unshielded twisted-pair cables by using electromagnetic topology techniques," [J]. *IEEE Transactions on Electromagnetic Compatibility*, vol. 63, pp. 125-140, 2006.

[17] C. Ye, E. Li, and Y. S. Gan, "Crosstalk for curvilinear conductors by utilising a nonuniform transmission line approach," [C]. *Electrical Performance of Electronic Packaging. IEEE*, pp. 189-192, 2001.

[18] R. Nevels and J. A. Miller, "Simple equation for analysis of nonuniform transmission lines," [J]. *IEEE Transactions on Microwave Theory & Techniques*, vol. 49, no. 4, pp. 721-724, 2002.

[19] C. R. Paul, Analysis of Multiconductor Transmission Lines. Wiley, pp. 45-54, 1994.

[20] A. Shoory, M. Rubinstein, A. Rubinstein, et al., "Application of the cascaded transmission line theory of Paul and McKnight to the evaluation of NEXT and FEXT in twisted wire pair bundles," [J]. *IEEE Transactions on Electromagnetic Compatibility*, vol. 55, no. 4, pp. 648-656, 2013.

[21] G. Li, G. Hess, R. Hoeckele, et al., "Measurement-based modeling and worst-case estimation of crosstalk inside an aircraft cable connector," [J]. *IEEE Transactions on Electromagnetic Compatibility*, vol. 57, no. 4, pp. 827-835, 2015.

[22] F. Loete, Q. Zhang, and M. Sorine, "Experimental validation of the inverse scattering method for distributed characteristic impedance estimation," [J]. *IEEE Transactions on Antennas & Propagation*, vol. 63, no. 6, pp. 2532-2538, 2015.

[23] F. Grassi, H. Abdollahi, G. Spadacini, et al., "Radiated immunity test involving crosstalk and enforcing equivalence with field-to-wire coupling," [J]. *IEEE Transactions on Electromagnetic Compatibility*, vol. 58, no. 1, pp. 1-9, 2015.

Pei Xiao was born in Shaoyang, Hunan province, China, in 1989. He received the bachelor and Ph.D. degrees in Mechanical Engineering from UESTC, Chengdu, China, in 2013 and 2019 respectively. He is currently a Postdoctoral Research Fellow in Research Center for Antennas and EMC, Hunan University.

His research interests are numerical computation, theoretical electromagnetic analysis including the EMT method, and EMC/EMI in Multi-conductor transmission line, power electronic device and electric vehicle.

Wan-Wei Ruan was born in Yiwu, Zhejiang province, China, in 1994. She received the B.E. from Huazhong Agricultural University in 2016.

She is currently a master student of UESTC. Her research interest is numerical methods of electromagnetic radiation and crosstalk.

Ping-An Du received the M.S. and Ph.D. degrees in Mechanical Engineering from Chongqing University, Chongqing, China, in 1989 and 1992, respectively.

He is currently a Full Professor of Mechanical Engineering at the University of Electronic Science and Technology of China, Chengdu, China. His research interests include numerical simulation in EMI, vibration, temperature, and so on.